

available at www.sciencedirect.comjournal homepage: www.elsevier.com/locate/biochempharm

Characterization of isoprostane signaling: Evidence for a unique coordination profile of 8-iso-PGF_{2α} with the thromboxane A₂ receptor, and activation of a separate cAMP-dependent inhibitory pathway in human platelets

Fadi T. Khasawneh¹, Jin-Sheng Huang, Fozia Mir, Subhashini Srinivasan, Chinnaswamy Tirupathi, Guy C. Le Breton^{*}

Department of Pharmacology, The University of Illinois at Chicago, 835 S Wolcott Avenue, M/C 868, Chicago, IL 60612, United States

ARTICLE INFO

Article history:

Received 30 January 2008

Accepted 24 March 2008

Keywords:

Thromboxane A₂ receptor

Isoprostanes

Platelet

Site-directed mutagenesis

Radioligand binding

Calcium mobilization

ABSTRACT

Since isoprostanes are thought to participate in the pathogenesis of thrombosis, presumably through their interaction with thromboxane receptors (TPRs), we examined the ability of 8-iso-PGF_{2α} to bind/signal through TPRs. Using TPR expressing HEK cells, it was found that 8-iso-PGF_{2α} mobilized calcium and bound TPRs with a dissociation constant (*K_d*) of 57 nM. Interestingly, site-directed-mutagenesis revealed that 8-iso-PGF_{2α} has a unique coordination profile with TPRs. Thus, while Phe¹⁸⁴ and Asp¹⁹³ are shared by both 8-iso-PGF_{2α} and classical TPR ligands, Phe¹⁹⁶ was found to be required only for 8-iso-PGF_{2α} binding. Functional studies also revealed interesting results. Namely, that 8-iso-PGF_{2α} signals in human platelets through both a stimulatory (TPR-dependent) and an inhibitory (cAMP-dependent) pathway. Consistent with the existence of two signaling pathways, platelets were also found to possess two separate binding sites for 8-iso-PGF_{2α}. While the stimulatory site is represented by TPRs, the second cAMP inhibitory site is presently unidentified, but does not involve receptors for PGI₂, PGD₂ or PGE₂. In summary, these studies provide the first documentation that: (1) 8-iso-PGF_{2α} coordinates with Phe¹⁸⁴, Asp¹⁹³ and Phe¹⁹⁶ on platelet TPRs; (2) Phe¹⁹⁶ serves as a unique TPR binding site for 8-iso-PGF_{2α}; (3) 8-iso-PGF_{2α} signals through both stimulatory and inhibitory pathways in platelets; (4) 8-iso-PGF_{2α} inhibits human platelet activation through a cAMP-dependent mechanism; (5) 8-iso-PGF_{2α} interacts with platelets at two separate binding sites. Collectively, these results provide evidence for a novel isoprostane function in platelets which is mediated through a cAMP-coupled receptor.

© 2008 Elsevier Inc. All rights reserved.

^{*} Corresponding author. Tel.: +1 312 996 4929; fax: +1 312 996 1225.

E-mail address: gcl@uic.edu (G.C. Le Breton).

¹ Current address: Department of Pharmaceutical Sciences, College of Pharmacy, Western University of Health Sciences, Pomona, CA 91766, United States.

Abbreviations: AA, arachidonic acid; AC, adenylate cyclase; cAMP, adenosine 3',5'-cyclic monophosphate; C-EL2, C-terminus of the second extracellular loop; HEK, human embryonic kidney; IPR, PGI₂ receptor; DPR, PGD₂ receptor; EP₂R, PGE₂ receptor; PRP, platelet rich plasma; ROCK, Rho-kinase; TRAP-PAR1, thrombin receptor-activating peptide 1; RT, room temperature; SC, shape change; TM5, the fifth transmembrane domain; TPR, thromboxane A₂ receptor; WT, wild type; AH 6809, 6-isopropoxy-9-oxoxanthene-2-carboxylic acid; BW A868C, 3-((2-cyclohexyl-2-hydroxyethyl)amino)-2,5-dioxo-1-(phenylmethyl)-4-benzyl-4-imidazolidine-heptanoic acid; CAY10441, (4S,5-dihydro-1H-imidazol-2-yl)-[4-(4-isopropoxy benzyl) phenyl] amine; 8-iso-PGF_{2α}, 9α, 11α, 15S-trihydroxy-(8β)-Prosta-5Z,13E-dien-1-oic acid; SQ29,548, [1S-[1α,2β(5Z),3β,4α]]-7-[3-[[2-[(phenyl-amino)carbonyl]hydrazino]methyl]-7-oxabicyclo[2.2.1]hept-2-yl]-5-heptenoic acid; U46619, 15(S)-hydroxy-11,9-epoxymethanoprostano-5Z,13E-dienoic acid.

0006-2952/\$ – see front matter © 2008 Elsevier Inc. All rights reserved.

doi:10.1016/j.bcp.2008.03.014

1. Introduction

The family of eicosanoids called isoprostanes possess a chemical structure that is isomeric to the classical prostanoids [1]. While the prostaglandins are produced as a result of cyclooxygenase enzyme activity, isoprostanes are generally thought to form nonenzymatically by free radical-mediated peroxidation of arachidonic acid (AA) [2]. Separate evidence has suggested that cyclooxygenase activity may also contribute to isoprostane production in selected tissues [3,4]. Of the isoprostane members, 8-iso-PGF_{2α} appears to be the most abundantly produced *in vivo* [1], and has been the most extensively studied.

After their initial identification, evidence was provided that isoprostanes may be involved in the development of certain disease states. For example, results obtained with an *in vivo* mouse model suggested that isoprostanes participate in thrombus development at sites of vascular injury [5]. Other studies found that the levels of isoprostanes become elevated in patients with atherosclerosis [6], acute myocardial infarction [7], as well as in a canine model of ischemia-reperfusion injury [7]. Regarding a possible role for isoprostanes in human brain disorders, it has been shown that isoprostanes are associated with the pathogenesis of Alzheimer's disease [8]. Finally, *in vitro* studies revealed that isoprostanes can induce oligodendrocyte progenitor cell death [9].

Due to the potential role of isoprostanes in the pathogenesis of disease, their cellular signaling pathways and biological effects have been under investigation. In this connection, isoprostanes were found to exert their biological activity in many cell types, e.g., platelets, vascular smooth muscle, kidney, etc., through TPR activation. For instance, it was found that 8-iso-PGF_{2α} caused platelet activation (shape change and reversible aggregation), that was sensitive to TPR antagonism [10,11]. In addition, a TPR antagonist was shown to block 8-iso-PGF_{2α}-induced vasoconstriction of vascular smooth muscle cells [12], carotid arteries [10], and renal glomeruli [13]. While recently disputed [10], the existence of discrete stimulatory isoprostane receptors in smooth muscle cells and human platelets has also been proposed [14–17]. This suggestion was based on differences between the potencies of 8-iso-PGF_{2α} and TPR agonists in inducing DNA synthesis [14] and MAP-kinase activation [15]. In summary, there are clear inconsistencies concerning the mechanisms by which isoprostanes modulate cellular function. Based on these considerations, we investigated three aspects of isoprostane biology: (1) their molecular interaction and signaling through TPRs; (2) their potential signaling through TPR-independent pathways; (3) their functional effects on human platelets and the mechanisms by which they produce these effects.

The initial experiments performed a comprehensive characterization of the interaction between 8-iso-PGF_{2α} and human TPRs using mutagenesis studies. Using 19 different TPR mutant cell lines, our data identified three key residues, i.e., Phe¹⁸⁴, Asp¹⁹³, and Phe¹⁹⁶ that are critical for 8-iso-PGF_{2α} binding. These data also revealed a coordination site between 8-iso-PGF_{2α} and TPRs, i.e., Phe¹⁹⁶, that is unique for 8-iso-PGF_{2α}. Moreover, our results provide evidence that human platelets possess two 8-iso-PGF_{2α} binding sites, which is consistent with the finding that 8-iso-PGF_{2α} signals through

two separate pathways (one stimulatory and one inhibitory). While the stimulatory signaling pathway is TPR-dependent, the inhibitory pathway is TPR-independent and associated with elevation of platelet cAMP levels.

2. Materials and methods

2.1. Reagents

The Fura2/AM dye was from Molecular Probes (Eugene, OR). [³H]8-iso-PGF_{2α}, 8-iso-PGF_{2α}, and other prostaglandins were from Cayman Chemical (Ann Arbor, MI). The Rho kinase inhibitor Y-27632, the phosphodiesterase inhibitor Ro20-1724, protein kinase A, protein kinase A inhibitor and Cellosolve were from Sigma (Saint Louis, MO). Cell culture supplies were from Fisher scientific (Hanover Park, IL). Human platelet concentrates were from Life Source Blood Services (Glenview, IL). [³H]cAMP was from Amersham Biosciences (Piscataway, NJ), and cold cAMP from Assay Designs (Ann Arbor, MI). ADP and TRAP-PAR1 peptide (SFLLRNPNDKYEPF) were from Research Genetics, (Huntsville, AL; now Invitrogen). The Adenylate cyclase inhibitor SQ22536 was from BIOMOL international (Plymouth Meeting, PA).

2.2. Cell lines stably expressing the wild type and site-directed mutations within the TPR sequence

A total of 20 different human embryonic kidney (HEK) cell lines with stable expression of the wild type and mutant TPRs were previously developed and characterized in our laboratory [18]. These cell lines possessed TPR expression levels that are comparable to the WT TPR cell line. Mutations were introduced at sites within the C-terminus of the second extracellular loop (C-EL2), or the fifth transmembrane domain (TM5).

2.3. Whole cell radioligand binding experiments

2.3.1. Saturation binding in HEK cells

These experiments were performed as previously described [18] with minor modifications to optimize binding for [³H]8-iso-PGF_{2α}. The cells were seeded on poly-L-lysine-coated 12 well plates. Upon confluency, the cells were washed twice with PBS, and then incubated with various predefined concentrations of [³H]8-iso-PGF_{2α} for 20 min at room temperature (RT) with gentle shaking. Next, the cells were rapidly washed once with PBS and 500 μl of 0.3N NaOH was added. The plates were shaken for 10 min at RT to detach the cells, and 100 μl of 3.0N HCl was added to neutralize the pH. The solubilized cell solution was then transferred to vials containing 8 ml of scintillation fluid, and counted in a Beckman LS 6500 liquid scintillation counter. To calculate the specific binding (which was approximately 60%), the same concentration of radioligand was competed against 1000-fold molar excess of unlabeled 8-iso-PGF_{2α}.

2.3.2. Saturation binding in intact platelets

Resuspended platelets were prepared as previously described in Ref. [19]. The PRP was treated with aspirin (1 mM) to inhibit endogenous platelet production of thromboxane A₂ (TXA₂), and centrifuged at 160 × g for 15 min to remove residual red

blood cells. PGI₂ (40 nM) was then added in order to aid in platelet resuspension. The PRP was then centrifuged at $1100 \times g$ for 15 min at 22 °C to pellet the platelets, and the pellet was resuspended in buffer (138 mM sodium chloride, 5 mM potassium chloride, 5 mM magnesium chloride, 5.5 mM glucose, and 25 mM Tris-HCl, pH 7.4). Platelets were counted and adjusted to a cell count of approximately 1×10^9 platelets/ml. The platelet suspension (1×10^9 platelets/ml) was incubated with predetermined concentrations of [³H]8-iso-PGF_{2α} for 20 min at RT. In order to conserve [³H]8-iso-PGF_{2α}, concentrations higher than 35 nM were supplemented with unlabelled 8-iso-PGF_{2α} (mixed-type binding curve). The specific binding was calculated in the presence of 1000-fold excess of the concentration of [³H]8-iso-PGF_{2α} used. Then, the [³H]8-iso-PGF_{2α} bound platelets were captured by vacuum filtration using 0.45 μm Millipore filters. The filters were rapidly washed once and counted for radioactivity. To calculate the specific binding (which was approximately 50%), the same concentration of radioligand was competed against 1000-fold molar excess of unlabeled 8-iso-PGF_{2α}. Of note, fit of the saturation binding experiments using a one-site versus a two-site model was compared using the F-test (PRISM version 4.0), which favored the two-binding site model.

2.3.3. Displacement binding in intact HEK cells/platelets

These experiments were performed similar to the saturation binding protocol with minor modifications. Briefly, platelets/HEK cells were incubated with 35 nM [³H]8-iso-PGF_{2α} at RT for 10 min. Increasing concentrations of the displacing ligand, i.e., 8-iso-PGF_{2α} (0.1 nM to 50 μM), SQ29,548 (0.1–5000 nM) or U46619 (0.035–50 μM) were then added for an additional 10 min, and samples were counted.

2.4. Cytosolic calcium measurements

These experiments were performed as previously described in Ref. [18]. Cells were loaded with 3 μM Fura2/AM for 25 min at 37 °C, and washed before stimulation with 8-iso-PGF_{2α}. The intracellular calcium was quantified by fluorescence imaging. For the inhibitor studies, cells were preincubated with 1 μM SQ29,548 at RT for approximately 10 min prior to stimulation with 8-iso-PGF_{2α}.

2.5. Human platelet functional studies

All of these experiments were conducted in freshly drawn PRP, and represent standard procedures for defining signaling mechanisms involved in platelet activation and inhibition.

2.5.1. Platelet shape change and aggregation

When platelets are activated, they first change their shape. This shape change involves a shift from smooth discoid-shaped cells to spherical cells with pseudopodia extending from their surface. This transition in shape significantly decreases the forward light scatter of the platelet suspension, and is manifest as a decrease in measured light transmittance through the sample. On the other hand, as platelets aggregate, the light transmission properties of the platelet suspension substantially increase due to the clustering of individual cells and the clearing of the suspension.

2.5.2. Platelet preparation and functional assay

Human platelet-rich plasma (PRP) was diluted with Tyrode's buffer to $2\text{--}3 \times 10^8$ platelets/ml, and incubated with 10 μM indomethacin for 2 min to prevent TXA₂ generation. PRP was then treated with either vehicle, U46619, 8-iso-PGF_{2α}, ADP, TRAP-PAR1, or the specific agonist/agent. The effects of these agents on shape change and aggregation were measured using the turbidimetric method [19,20] with a model 400 aggregometer (Chrono-Log; Havertown, PA). For the inhibitor studies, PRP was incubated with a predetermined dose of the drug for 1 min prior to stimulation with 8-iso-PGF_{2α} or U46619. The 8-iso-PGF_{2α} aggregation enhancement studies were performed by preincubating the PRP with 8-iso-PGF_{2α} and then stimulation with agonist. The 8-iso-PGF_{2α} aggregation inhibition studies were done by incubating PRP with SQ29,548 for 1 min, then 8-iso-PGF_{2α} for 3 min, followed by stimulation with agonist. Furthermore, the reversal of this inhibition was performed in a similar manner but after incubation with the adenylate cyclase inhibitor SQ22536 for 45 min.

2.6. Assay of platelet adenosine 3',5'-cyclic monophosphate (cAMP)

Human PRP (500 μl) samples were collected in an Eppendorf tube and treated with vehicle, PGI₂, 8-iso-PGF_{2α} (with or without SQ22536), antagonists, and/or agonists. Next, the phosphodiesterase inhibitor RO20-1724 (100 μM) was added, and platelets were spun down and immediately frozen in liquid nitrogen. The platelet pellet was then resuspended, sonicated, boiled for 4 min, spun down, and the supernatant was transferred to a new tube. The concentration of cAMP in the supernatant was measured as previously described in Refs. [21,22]. The standard curve samples were prepared by adding known concentrations of unlabeled cAMP to the supernatant obtained from vehicle treated platelets. Its note worthy that 8-iso-PGF_{2α} failed to increase cAMP in the non-transfected or wild-type TPR expressing HEK cells.

2.7. Analysis of data

All experiments were performed at least three times, and platelet studies used PRP from at least three different donors. Data were analyzed using GraphPad PRISM statistical software (San Diego, CA) and presented as mean ± standard error of the mean (S.E.M.). While the saturation binding isotherms and the Scatchard plot were generated using non-linear regression analysis, the standard cAMP curve was generated by applying linear regression. Results were compared using unpaired two-tailed Student's t-test, with $p < 0.05$ considered to be statistically significant.

3. Results

3.1. Binding and signaling of 8-iso-PGF_{2α} through TPRs

In order to fully characterize the biology of 8-iso-PGF_{2α} and to address previous inconsistencies concerning its signaling properties [10,14], we first investigated its binding capacity to TPRs and its functional activation of these receptors using a

stable cell line expressing TPRs. Our initial studies demonstrated that the non-TPR transfected HEK cells neither bound [3 H]8-iso-PGF $_{2\alpha}$ nor exhibited detectable calcium (Ca^{2+}) mobilization in response to 8-iso-PGF $_{2\alpha}$ (5 μM ; not shown). Next, we performed experiments on the wild-type (WT) TPR stable HEK cell line, which was previously characterized in our laboratory [18]. The results revealed a single 8-iso-PGF $_{2\alpha}$ binding site with a dissociation constant (K_d) of 57 ± 7 nM (Fig. 1A and Table 1), and that receptor saturation was achieved at approximately 200 nM. Interestingly, this K_d is almost an order of magnitude lower than the value previously reported for this ligand [15]. Functional analysis demonstrated that 8-iso-PGF $_{2\alpha}$ resulted in robust Ca^{2+} mobilization (Fig. 1B and Table 1), and that the maximal response was obtained with 250 nM of 8-iso-PGF $_{2\alpha}$ (Fig. 1B inset). This Ca^{2+} response was found to be TPR mediated, since it was blocked by the antagonist SQ29,548 (Fig. 1C). Furthermore, displacement-binding studies revealed

that 1 μM of the TPR antagonist SQ29,548, or 10 μM of the TPR agonist U46619 completely displaced [3 H]8-iso-PGF $_{2\alpha}$ binding to TPRs (Fig. 1D and E). Taken together, these data indicate that 8-iso-PGF $_{2\alpha}$ has the capacity to bind and signal in TPR-transfected HEK cells.

We next sought to identify the amino acid residues which mediate isoprostane-TPR coordination by employing site-directed-mutagenesis. These experiments employed 19 separate HEK cell lines stably expressing mutant TPRs [18]. These mutant receptors substitute the parent amino acid with at least two other residues of different chemical properties. In each of these analyses, the mutant cells were characterized for TPR surface expression by flow cytometry analysis [18], for ligand binding to [3 H]8-iso-PGF $_{2\alpha}$, and for 8-iso-PGF $_{2\alpha}$ -induced calcium mobilization. Thus, these studies represented a comprehensive investigation of 8-iso-PGF $_{2\alpha}$ coordination with the TPR ligand-binding domain.

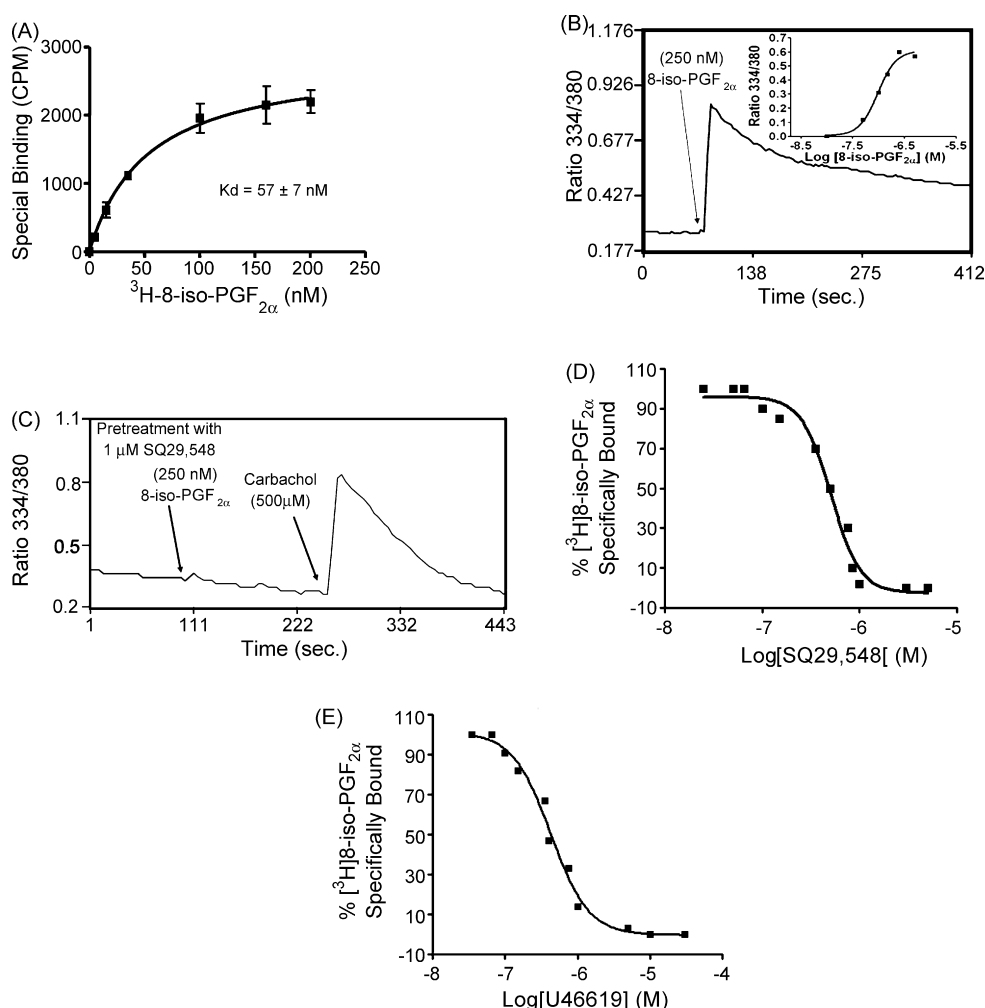


Fig. 1 – Characterization of a stable wild-type TPR expressing HEK cell line for 8-iso-PGF $_{2\alpha}$ coordination. Cells were evaluated using radioligand binding and calcium mobilization. (A) Saturation binding isotherm using [3 H]8-iso-PGF $_{2\alpha}$. Cells were incubated with various concentrations of [3 H]8-iso-PGF $_{2\alpha}$ to generate the saturation binding isotherm. (B) 250 nM 8-iso-PGF $_{2\alpha}$ -induced Ca^{2+} mobilization (inset shows dose-response curve of 8-iso-PGF $_{2\alpha}$ -induced Ca^{2+} mobilization). (C) Blockade of 8-iso-PGF $_{2\alpha}$ -induced Ca^{2+} mobilization using SQ29,548. Cells were also treated with carbachol as a control. (D) Binding displacement of 35 nM [3 H]8-iso-PGF $_{2\alpha}$ with increasing concentrations of SQ29,548 (0.025–5 μM). (E) Binding displacement of 35 nM [3 H]8-iso-PGF $_{2\alpha}$ with increasing concentrations of U46619 (0.035–30 μM). Results are the average (A, D and E), or representative (B and C) of at least three different experiments.

Table 1 – A summary of the 8-iso-PGF_{2α} binding ($K_d \pm$ S.E.M.), B_{max} (\pm S.E.M.) and Ca²⁺ mobilization data for the wild type, and the mutant TPR expressing cell lines, as well as for platelets

Cell line	8-Iso-PGF _{2α} K_d (nM)	Calcium mobilization	B_{max}
WT	57 \pm 7	+++	2855 \pm 237
F184A*	NA	None	NA
F184Y*	NA	None	NA
T186A	43 \pm 10	+++	2470 \pm 315
T186S	71 \pm 6	+++	3016 \pm 416
E190A	62 \pm 8	+++	2890 \pm 364
E190D	55 \pm 6	+++	2033 \pm 234
S191A	65 \pm 5	+++	2636 \pm 252
S191T	53 \pm 7	+++	2243 \pm 218
D193N	69 \pm 7	+++	2388 \pm 176
D193A*	NA	None	NA
D193E	74 \pm 3	+++	2198 \pm 180
D193Q*	NA	None	NA
D193R*	NA	None	NA
F196A*	NA	None	NA
F196Y	53 \pm 5	+++	2110 \pm 316
F200A	60 \pm 6	+++	2375 \pm 321
F200Y	42 \pm 8	+++	2147 \pm 291
S201A	66 \pm 9	+++	2094 \pm 272
S201T	60 \pm 3	+++	2504 \pm 323
Platelets	(1) 65 \pm 5 (2) 322 \pm 29	NA NA	(1) 3420 \pm 345 (2) 2712 \pm 221

Results are the average of at least three different experiments in each case (* $p < 0.05$). NA, not applicable.

3.2. Aspartic acid 193 (Asp¹⁹³) engages in hydrogen bonding with 8-iso-PGF_{2α}

Since our previous work demonstrated that Asp¹⁹³ plays a critical role in TPR–ligand interaction [18], it was the first site to be evaluated. In order to define the nature of the coordination force between Asp¹⁹³ and 8-iso-PGF_{2α}, this site was substituted by five different residues. Specifically, Asp¹⁹³ was replaced by alanine (D193A; elimination of the side chain); glutamine (D193Q; concomitant insertion of a methylene group and substitution of the COOH with NH₂) and; arginine (D193R; charge reversal). The results demonstrated that none of the mutants (D193A/Q/R) exhibited detectable binding to [³H]8-iso-PGF_{2α}, even at a concentration that normally saturates the WT TPR, i.e., 200 nM (Fig. 2A, Table 1, and not shown). In addition, these mutants also lost the 8-iso-PGF_{2α}-induced Ca²⁺ mobilization response, even at 5 μM (Fig. 2B, Table 1, and not shown). Hence, 8-iso-PGF_{2α} coordination at the 193 position is not supported by any of the aforementioned changes in the chemistry of this site. On the other hand, both binding and function were maintained when the Asp¹⁹³ was changed to glutamic acid (D193E; insertion of a methylene group) or asparagine (D193N; substitution of the COOH with NH₂) (Fig. 2C–F and Table 1). Taken together, these findings indicate that Asp¹⁹³ coordination with 8-iso-PGF_{2α} is similar to that for SQ29,548 and U46619 [18], i.e., hydrogen bonding in nature, and depends on the length of the amino acid side-chain, its charge characteristics, and its conformation.

3.3. Phenylalanine 184 (Phe¹⁸⁴) coordinates with 8-iso-PGF_{2α} using hydrophobic forces

We next investigated whether Phe¹⁸⁴ is also involved in 8-iso-PGF_{2α} binding. In order to define the nature of the binding force

at this site, tyrosine and alanine (i.e. F184Y/A) mutations were separately introduced. Experiments demonstrated that neither mutant significantly bound to [³H]8-iso-PGF_{2α} nor mobilized Ca²⁺ in response to 8-iso-PGF_{2α} (Fig. 3A and B, Table 1, and not shown). These findings provide evidence that Phe¹⁸⁴ plays a critical role in isoprostane coordination, and that the binding forces are similar to those previously reported for SQ29,548 and U46619, i.e., hydrophobic [18]. Furthermore, since the tyrosine substitution at this site was also incapable of supporting coordination with 8-iso-PGF_{2α}, these hydrophobic forces seem to require certain conformational characteristics.

The next set of experiments evaluated the participation of other C-EL2 residues in 8-iso-PGF_{2α} binding. Specifically, glutamic acid (Glu¹⁹⁰) was substituted with alanine or aspartic acid (E190A/D); threonine (Thr¹⁸⁶) was replaced with serine or alanine (T186S/A); and serine (Ser¹⁹¹) was mutated to alanine or threonine (S191A/T). The data revealed that none of the aforementioned mutations produced any detectable effect on 8-iso-PGF_{2α} binding or functional response (Table 1). Therefore, these results indicate that Glu¹⁹⁰, Thr¹⁸⁶, and Ser¹⁹¹ do not participate in 8-iso-PGF_{2α}–TPR coordination. Subsequent studies determined whether sites within the fifth transmembrane (TM5) region of TPRs might also be involved in 8-iso-PGF_{2α} binding.

3.4. Binding sites for 8-iso-PGF_{2α} within TM5: a role for Phe¹⁹⁶

The first amino acid selected for analysis within TM5 was Phe¹⁹⁶. It was found that substitution of this residue with alanine, i.e., F196A, resulted in a loss of both [³H]8-iso-PGF_{2α} binding activity (Fig. 4A and Table 1), and the capacity of 8-iso-PGF_{2α} to mobilize Ca²⁺ (Fig. 4B and Table 1), whereas it produced no effect on binding of TPR ligands such as SQ29,548

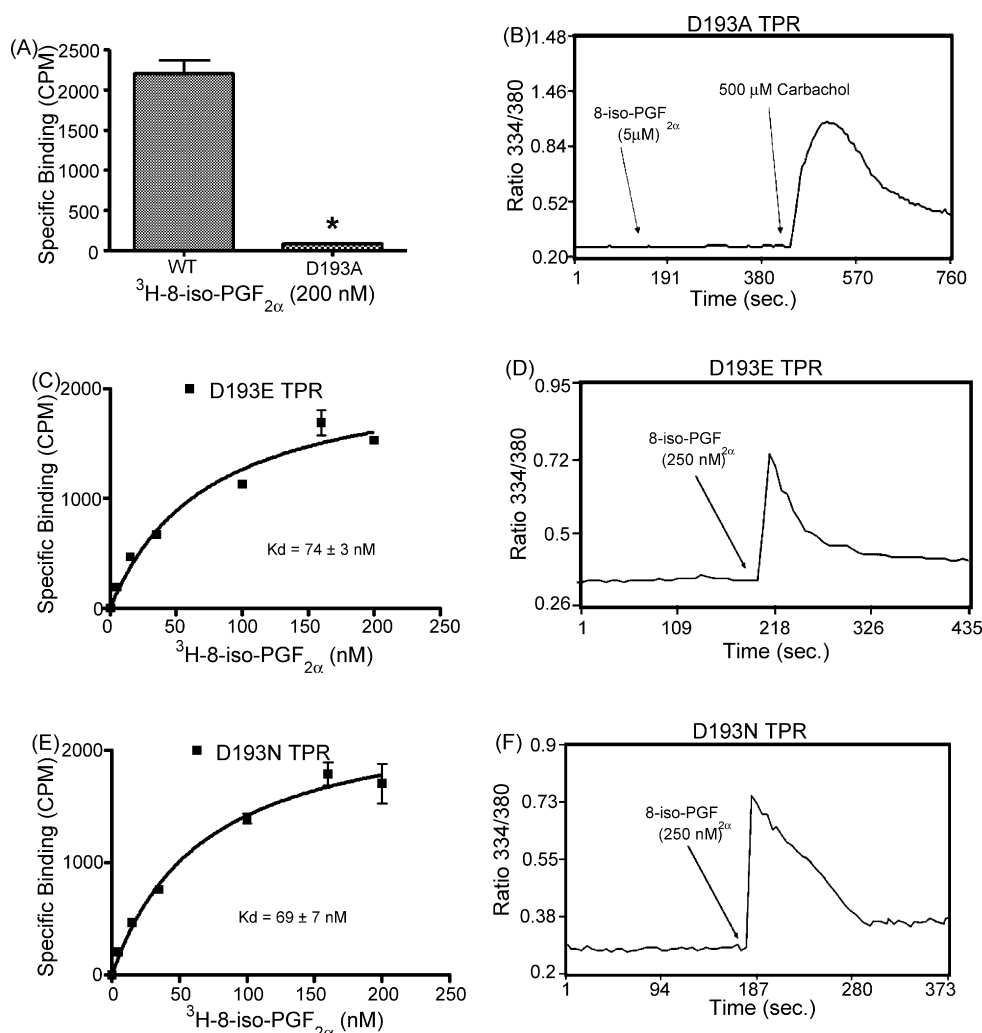


Fig. 2 – Aspartic acid 193 mutations: alanine (D193A), glutamic acid (D193E), and asparagine (D193N). Cells were evaluated using radioligand binding and calcium mobilization. (A) Binding of [^3H]8-iso-PGF $_{2\alpha}$ to D193A cells. Bar graph represents binding of 200 nM of [^3H]8-iso-PGF $_{2\alpha}$ (a concentration that saturates wild-type TPR) ($p < 0.05$, $n = 3$). (B) 5 μM 8-iso-PGF $_{2\alpha}$ -induced Ca^{2+} mobilization. D193A cells were also treated with carbachol as a control. (C) Saturation binding isotherm for D193E using [^3H]8-iso-PGF $_{2\alpha}$. Cells were incubated with various concentrations of [^3H]8-iso-PGF $_{2\alpha}$ to generate the saturation binding isotherm. (D) 250 nM 8-iso-PGF $_{2\alpha}$ -induced Ca^{2+} mobilization for D193E. (E) Saturation binding isotherm for D193N using [^3H]8-iso-PGF $_{2\alpha}$. Cells were incubated with various concentrations of [^3H]8-iso-PGF $_{2\alpha}$ to generate the saturation binding isotherm. (F) 250 nM 8-iso-PGF $_{2\alpha}$ -induced Ca^{2+} mobilization in D193N. Results are the average (A, C, and D) or representative (B, D, and F) of at least three different experiments.

and U46619 [18]. Since the alanine mutation removed the benzene side chain of Phe 196 , these findings suggest that the interaction force between 8-iso-PGF $_{2\alpha}$ and this site is hydrophobic in nature. This notion was verified by mutating Phe 196 to tyrosine (i.e. F196Y), which still contains the benzene group, and hence hydrophobic bonding capability. Our data revealed that the F196Y cells possessed an isoprostane binding affinity ($K_d = 53 \pm 5$ nM; Fig. 4C and Table 1), and a Ca^{2+} response which were comparable to WT TPRs (Fig. 4D and Table 1). Also, the functional response was blocked by SQ29,548 (not shown). Taken together, this result suggests that hydrophobic forces are responsible for coordination of the benzene ring of Phe 196 with 8-iso-PGF $_{2\alpha}$.

We next evaluated Ser 201 and Phe 200 mutations, i.e., S201A/T and F200A/Y. The results demonstrated that all of these mutations exhibited a WT phenotype for both binding of [^3H]8-iso-PGF $_{2\alpha}$ and its functional response (Table 1). Consequently, neither Ser 201 nor Phe 200 seem to be involved in 8-iso-PGF $_{2\alpha}$ interaction with TPRs.

In summary, while Glu 190 , Thr 186 , Ser 191 , Ser 201 and Phe 200 do not appear to be important for 8-iso-PGF $_{2\alpha}$ coordination with TPRs, Phe 196 , Asp 193 , and Phe 184 were identified to be critical for this ligand interaction. Furthermore, the results obtained with the Phe 196 TPR mutants demonstrate that 8-iso-PGF $_{2\alpha}$ has a different amino acid coordination profile than classical TPR ligands. In the next series of experiments we

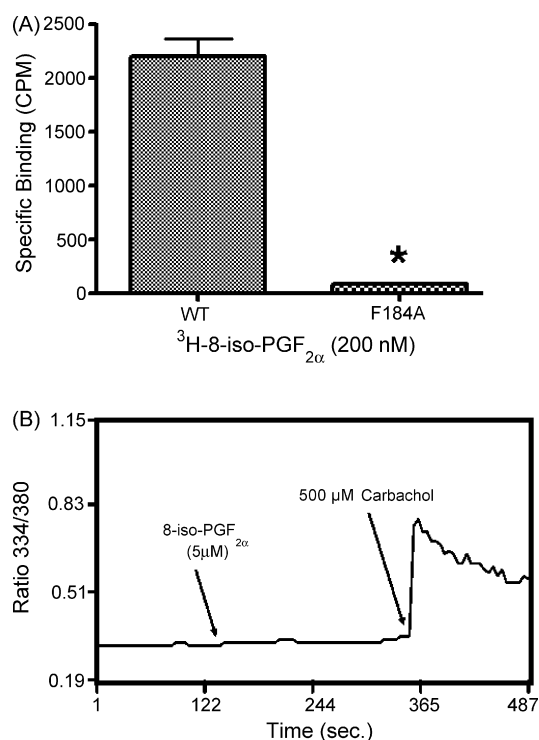


Fig. 3 – The phenylalanine 184 to alanine mutation (F184A). Cells were evaluated using radioligand binding and calcium mobilization. (A) Binding of [³H]8-iso-PGF_{2α} to F184A. Bar graph represents binding of 200 nM of [³H]8-iso-PGF_{2α}. Results are representative of the average of at least three different experiments ($p < 0.05$, $n = 3$). (B) 5 μM 8-iso-PGF_{2α}-induced Ca²⁺ mobilization in F184A ($p < 0.05$, $n = 3$). Cells were also treated with carbachol as a control. Results are the average (A), or representative (B) of at least three different experiments in each case ($p > 0.05$, $n = 3$).

extended our investigation of isoprostane signaling to a native-TPR cell system, i.e., human blood platelets.

3.5. Effects of 8-iso-PGF_{2α} on human blood platelets function

3.5.1. Shape change

Our results demonstrated that addition of U46619 (0.5 μM) to human PRP produced a typical shape change (SC) and aggregation response (Fig. 5A). In contrast, it was found that 8-iso-PGF_{2α} stimulated platelet SC, but not aggregation, even at concentrations as high as 5 μM (Fig. 5B and Fig. 5B inset). Dose-response analysis revealed that 50 nM SQ29,548 was required to completely block U46619-induced aggregation (Fig. 5A inset), and the 8-iso-PGF_{2α}-mediated SC response (Fig. 5C). This finding suggests that 8-iso-PGF_{2α}-mediated SC proceeds through a TPR-mediated process. Furthermore, it was also found that the Rho-kinase (ROCK) inhibitor Y-27632 dose-dependently inhibited 8-iso-PGF_{2α}-induced SC (Fig. 5D), indicating that ROCK activation is necessary for this functional response.

Interestingly, even though 8-iso-PGF_{2α} signals through TPRs, it was itself incapable of stimulating platelet aggregation (Fig. 5B). Indeed, previous results have demonstrated that 8-

iso-PGF_{2α} has the capacity to inhibit aggregation stimulated by U46619 [11,23]. While the reason for this peculiar biological profile is unknown, it may derive from partial agonist activity at TPRs (as has been previously proposed) [23], or the ability of 8-iso-PGF_{2α} to simultaneously stimulate TPRs and a separate inhibitory signaling pathway. The next series of experiments were designed to examine each of these possibilities.

3.5.2. Enhancement of platelet aggregation induced by ADP or TRAP-PAR1

If 8-iso-PGF_{2α} acts as a partial agonist through TPRs, one might expect 8-iso-PGF_{2α} enhancement of platelet aggregation in response to non-TPR agonists, e.g., ADP and TRAP-PAR1. Our results demonstrated that pretreating platelets with 8-iso-PGF_{2α} (1 μM) did in fact enhance aggregation in response to 10 μM ADP (Fig. 6A traces a and b) and 15 μM TRAP-PAR1 (Fig. 6B traces a and b), which is consistent with partial agonist activity for 8-iso-PGF_{2α}. If this is in fact correct, it would be expected that inhibition of TPR signaling should block this enhanced response. This notion was examined in the next series of experiments.

3.5.3. Inhibition of platelet aggregation in response to ADP or TRAP-PAR1 in the presence of the TPR antagonist SQ29,548

In the initial studies, it was found that treatment with SQ29,548 did not affect platelet aggregation induced by either ADP (Fig. 6A trace c) or TRAP-PAR1 (Fig. 6B trace c). On the other hand, addition of 8-iso-PGF_{2α} in the presence of SQ29,548 produced approximately 50% inhibition of the aggregation response induced by ADP (Fig. 6A trace d) or TRAP-PAR1 (Fig. 6B trace d). Thus, in the absence of TPR signaling, 8-iso-PGF_{2α} was no longer found to enhance aggregation. Indeed, under these conditions an inhibitory component of 8-iso-PGF_{2α} signaling is revealed. Collectively, these results suggest that 8-iso-PGF_{2α} signals through two pathways with opposing biological activities: a TPR-mediated stimulatory pathway; and an unidentified pathway which is inhibitory in nature. The following set of experiments was designed to characterize this inhibitory signaling pathway for 8-iso-PGF_{2α}.

3.6. Effects of 8-iso-PGF_{2α} on platelet cAMP levels

Since cAMP is a known inhibitor of platelet function, subsequent experiments measured the ability of 8-iso-PGF_{2α} to alter platelet cAMP levels. It can be seen (Fig. 6C) that treatment of PRP with 8-iso-PGF_{2α} (0.1–7.5 μM) dose-dependently increased platelet cAMP, and that this increase was not sensitive to blockade by SQ29,548, even at 1 μM of this TPR antagonist (Fig. 6C). These findings provide evidence that 8-iso-PGF_{2α} raises platelet cAMP levels through a TPR-independent mechanism, and suggest that this mechanism serves as the 8-iso-PGF_{2α} inhibitory component. This result is in marked contrast to the effects of 8-iso-PGF_{2α} on cAMP levels in HEK cells, which revealed no increase in cAMP upon 8-iso-PGF_{2α} addition (even in cells transfected with TPRs), as compared with the control forskolin (Fig. 6G). This finding is particularly interesting, since it indicates that the underlying mechanism of cAMP elevation in platelets does not involve direct activation of either adenylate cyclase (AC) or G_{αs}, both of which are present in HEK cells [24].

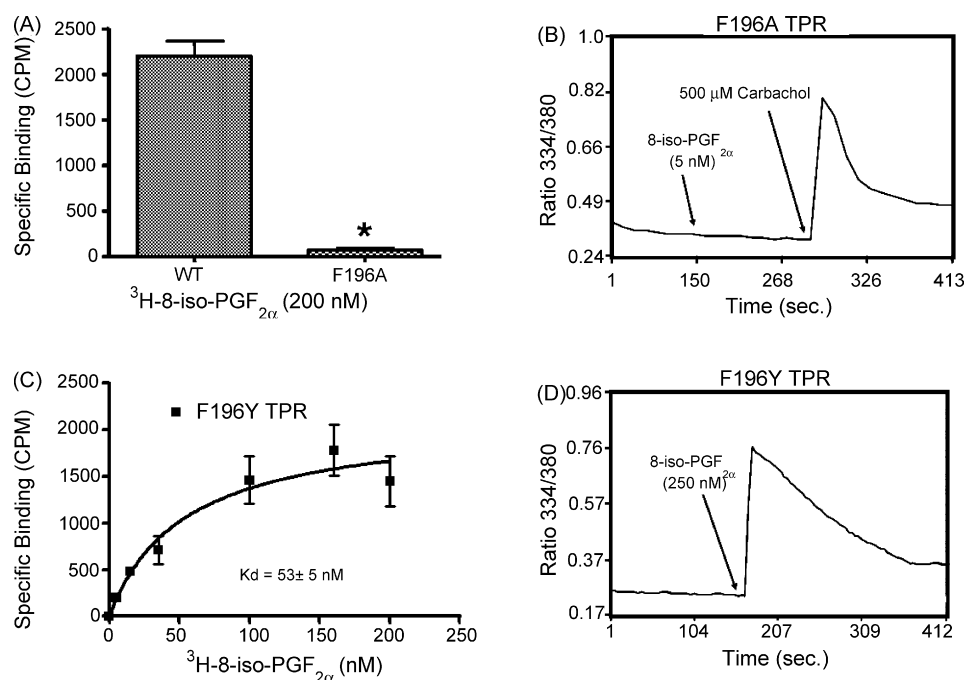


Fig. 4 – Phenylalanine 196 mutations: alanine (F196A) and tyrosine (F196Y). Cells were evaluated using radioligand binding and calcium mobilization. (A) Binding of [^3H]8-iso-PGF $_{2\alpha}$ to F196A. Bar graph represents binding of 200 nM of [^3H]8-iso-PGF $_{2\alpha}$ ($p < 0.05$, $n = 3$). (B) 5 μM 8-iso-PGF $_{2\alpha}$ -induced Ca^{2+} mobilization in F196A ($p < 0.05$, $n = 3$). Cells were also treated with carbachol as a control. (C) Saturation binding isotherm for F196Y using [^3H]8-iso-PGF $_{2\alpha}$. Cells were incubated with various concentrations of [^3H]8-iso-PGF $_{2\alpha}$ to generate the saturation binding isotherm. (D) 250 nM 8-iso-PGF $_{2\alpha}$ -induced Ca^{2+} mobilization in F196Y. Results are the average (A and C), or representative of at least three different experiments (B and D) ($p > 0.05$, $n = 3$).

In order to support the notion that 8-iso-PGF $_{2\alpha}$ -induced increases in platelet cAMP are responsible for the observed inhibition of platelet function, a permeable AC inhibitor SQ22536 was employed. In order to establish the effectiveness of SQ22536, control experiments were first conducted with PGI $_2$ which is known to produce its inhibitory effects through AC activation. It can be seen that SQ22536 effectively reversed PGI $_2$ -inhibition of ADP- or TRAP-PAR1-induced platelet aggregation (Fig. 6D and not shown), and blocked the ability of PGI $_2$ to raise platelet cAMP levels (Fig. 6C). Similarly, SQ22536 produced a complete reversal of 8-iso-PGF $_{2\alpha}$ inhibition of aggregation (Fig. 6E and F) and its associated increase in cAMP (Fig. 6C). Taken together, these results provide evidence that 8-iso-PGF $_{2\alpha}$ has the capacity to raise platelet cAMP, and that this increase in cAMP serves as the mechanism underlying its blockade of human platelet aggregation that is revealed in the presence of SQ29,548. The next experiments investigated whether 8-iso-PGF $_{2\alpha}$ increases cAMP through activation of known Gs coupled prostaglandin receptors on platelets.

3.7. 8-Iso-PGF $_{2\alpha}$ raises cAMP independent of the receptors for PGI $_2$, PGD $_2$, and PGE $_2$

In order to determine whether 8-iso-PGF $_{2\alpha}$ activates the receptors for PGI $_2$ (IPR), PGD $_2$ (DPR) or PGE $_2$ (EP $_2$ R), antagonists specific to each of these receptors were employed, i.e., CAY10441 (IPR specific) [25]; BW A868C (DPR specific) [26]; and AH 6809 (EP $_2$ R specific) [27]. Consistent with their reported

specificity, the results demonstrated that each of these antagonists only inhibited cAMP production (Fig. 7A), and reversed inhibition of aggregation in response to activation of its corresponding receptor (Fig. 7B–D and not shown). Moreover, none of the antagonists produced any detectable effects on the cAMP levels elevated by 8-iso-PGF $_{2\alpha}$ (Fig. 7E), or on its ability to inhibit ADP- or TRAP-PAR1-induced aggregation (Fig. 7F and not shown). These findings suggest that 8-iso-PGF $_{2\alpha}$ increases cAMP, and inhibits platelet function through a mechanism independent of IPR, DPR or EP $_2$ R activation.

A separate mechanism by which 8-iso-PGF $_{2\alpha}$ raises platelet cAMP may involve a distinct G $_{\alpha s}$ -coupled receptor for isoprostanes, or a novel interaction with a known receptor other than IPR, DPR and EP $_2$ R. If this is the case, then 8-iso-PGF $_{2\alpha}$ would be expected to interact with human platelets at two separate binding sites. This possibility was investigated in the following experiments.

3.8. 8-Iso-PGF $_{2\alpha}$ possesses two binding sites in intact platelets

Using radioligand displacement studies, it was found that non-radiolabeled 8-iso-PGF $_{2\alpha}$ completely displaced [^3H]8-iso-PGF $_{2\alpha}$ from its binding sites (Fig. 8A). On the other hand, this finding is in marked contrast to SQ29,548 or U46619 which only partially competed for [^3H]8-iso-PGF $_{2\alpha}$ binding to human platelets (Fig. 8B and C), i.e., there was 40% residual isoprostane binding in the presence of excess SQ29,548 or

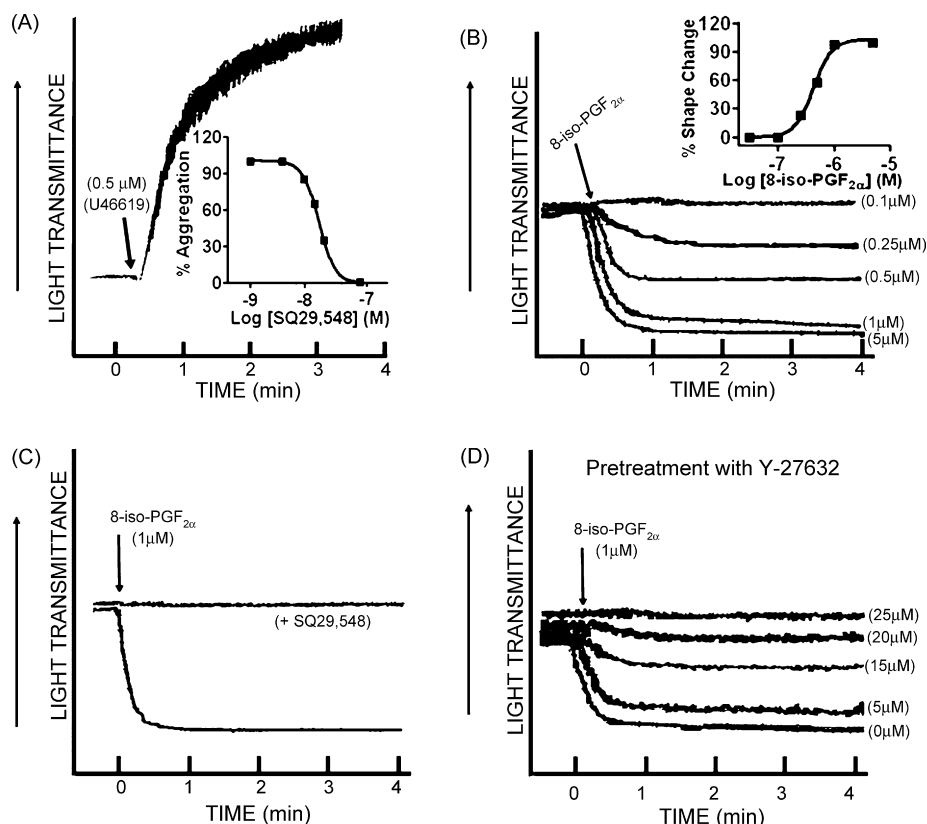


Fig. 5 – Effects of U46619 and 8-iso-PGF_{2α} on human platelets in the presence or absence of SQ29,548 or Y-27632. (A) PRP was stimulated with 0.5 μM U46619 (inset shows dose-dependent inhibition curve of U46619-induced aggregation by the TPR antagonist SQ29,548). (B) PRP was stimulated with various concentrations of 8-iso-PGF_{2α} (0.1–5 μM; inset shows dose-response curve of 8-iso-PGF_{2α}-induced platelet shape change). (C) PRP was stimulated with 1 μM 8-iso-PGF_{2α} in the presence or absence of 50 nM SQ29,548. (D) PRP was stimulated with 1 μM 8-iso-PGF_{2α} in the presence of increasing concentrations of the ROCK inhibitor Y-27632 (5–25 μM). Each aggregation curve is representative of multiple traces obtained from three separate platelet preparations.

U46619. The nature of this residual binding was revealed in saturation binding experiments, which demonstrated the existence of two distinct affinity sites for [³H]8-iso-PGF_{2α} on human platelets; one with a $K_d = 65 \pm 5$ nM, and a second with a $K_d = 322 \pm 29$ nM (Fig. 8D, inset and Table 1). The presence of two binding sites was further confirmed by generating a B/B_0 versus Log [8-iso-PGF_{2α}] plot. Using F-test analysis, a two-site model of this plot was found to be favored (Fig. 8E).

In summary, the above results demonstrate that 8-iso-PGF_{2α} coordinates with TPRs through three key amino acids, i.e., Phe¹⁸⁴, Asp¹⁹³, and Phe¹⁹⁶, and that Phe¹⁹⁶ represents a unique binding site which is not shared with classical TPR ligands, e.g. U46619 and SQ29,548. These results also provide evidence that 8-iso-PGF_{2α} interacts with platelets at two different binding sites, and simultaneously signals through a stimulatory (TPR-dependent) and an inhibitory (cAMP-dependent) pathway.

4. Discussion

Despite ample evidence supporting a potential role for isoprostanes in disease processes such as apoptosis, brain

cell damage, and thrombosis, their biological activity and signaling mechanisms are poorly understood. Nevertheless, certain evidence has suggested that 8-iso-PGF_{2α} can signal through TPRs. For example, the use of TPR antagonists provided evidence that 8-iso-PGF_{2α} stimulates platelet shape change and/or weak aggregation through a TPR-mediated process [14,15,23]. In contrast, other results are inconsistent with the notion that the stimulatory effects of 8-iso-PGF_{2α} are mediated through TPRs [16,17]. While the reasons for these apparent discrepancies are not known, they may derive from variations in the experimental conditions/cellular preparations, or inherent differences in the potency of the ligands employed.

To further investigate 8-iso-PGF_{2α} signaling mechanisms, a stable cell line expressing the WT TPR was examined. It was found that [³H]8-iso-PGF_{2α} bound to HEK TPRs at a single site, and that this binding was completely displaced by either SQ29,548 or U46619. Furthermore, saturation binding analysis revealed a K_d (57 nM) for [³H]8-iso-PGF_{2α} that is substantially lower than that previously reported [15]. One possible reason for this affinity difference may derive from TPR expression levels, which we have shown to affect receptor ligand affinity [28].

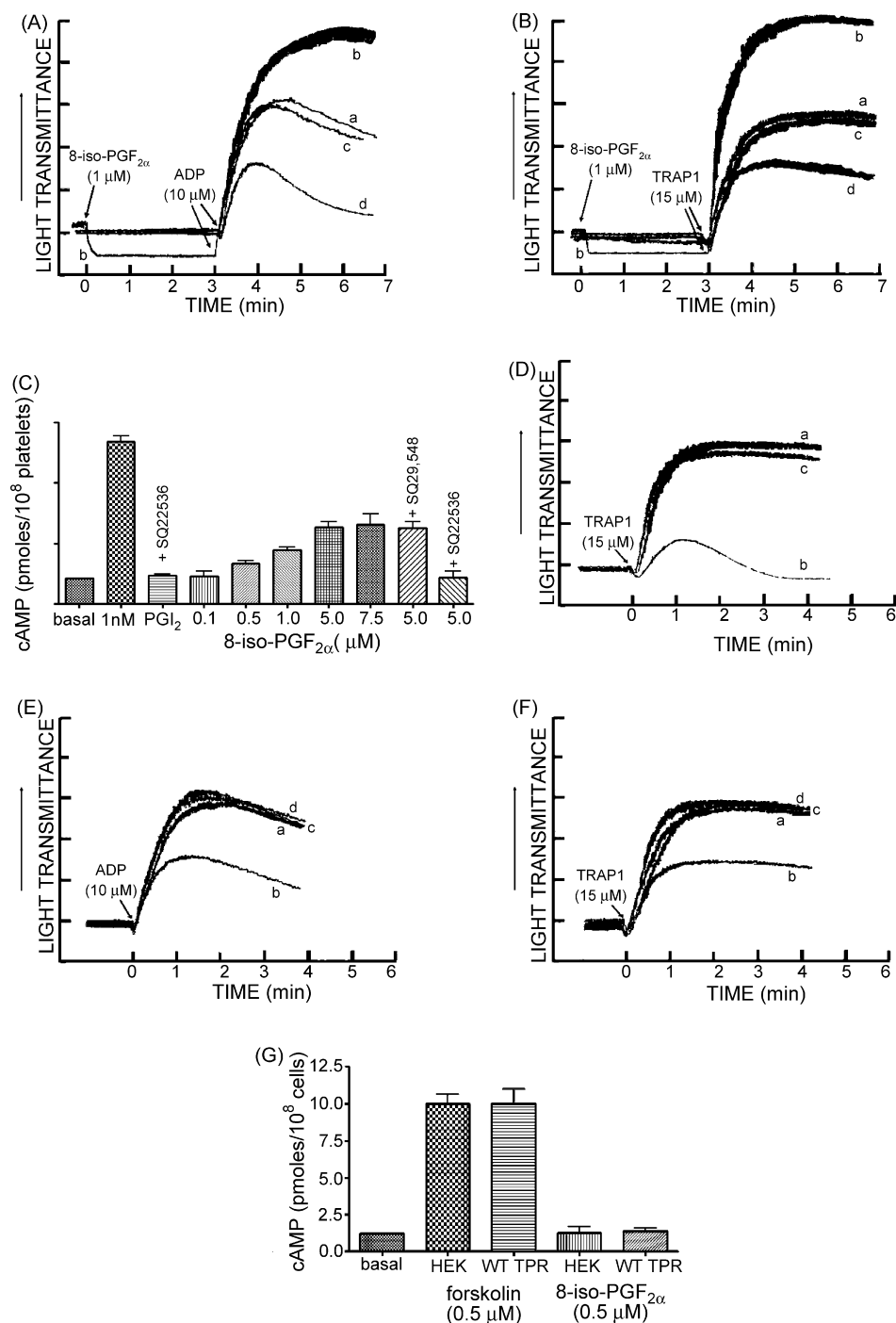


Fig. 6 – Effects of 8-iso-PGF_{2α} or PGI₂ on human platelet aggregation induced by ADP or TRAP-PAR1 in the presence or absence of the AC inhibitor SQ22536; and effects of PGI₂, 8-iso-PGF_{2α}, or forskolin on basal cAMP levels in human platelets and/or HEK cells in the presence or absence of SQ29,548. (A) trace (a) PRP was stimulated with 10 μM ADP; trace (b) PRP was treated with 1 μM 8-iso-PGF_{2α} for 3 min prior to stimulation with 10 μM ADP; trace (c) PRP was treated with 50 nM SQ29,548 for 1 min prior to stimulation with 10 μM ADP; trace (d) PRP was treated with 50 nM SQ29,548 for 1 min, then with 1 μM 8-iso-PGF_{2α} for 3 min prior to stimulation with 10 μM ADP. (B) trace (a) PRP was stimulated with 15 μM TRAP-PAR1; trace (b) PRP was treated with 1 μM 8-iso-PGF_{2α} for 3 min prior to stimulation with 15 μM TRAP-PAR1; trace (c) PRP was treated with 50 nM SQ29,548 for 1 min prior to stimulation with 15 μM TRAP-PAR1; trace (d) PRP was treated with 50 nM SQ29,548 for 1 min, then with 1 μM 8-iso-PGF_{2α} for 3 min prior to stimulation with 15 μM TRAP-PAR1. (C) PRP was treated with various concentrations of 8-iso-PGF_{2α} (0.1–7.5 μM) or 1 nM of the control PGI₂ in the presence or absence of the AC inhibitor SQ22536 or 1 μM of the TPR antagonist SQ29,548. (D) trace (a) PRP was stimulated with 15 μM TRAP-PAR1; trace (b) PRP was treated with 50 nM SQ29,548 for 1 min, then with 1 μM 8-iso-PGF_{2α} for 3 min prior to stimulation with 15 μM TRAP-PAR1; trace (c) PRP was stimulated with 15 μM TRAP-PAR1 after incubation with the AC inhibitor SQ22536 (300 μM) for 45 min; trace (d)

We next sought to identify the amino acid residues (in C-EL2 and TM5) that mediate the isoprostane–TPR interaction process. This was accomplished by analyzing the effect of 19 different substitutions (in the TPR ligand binding domain) on 8-iso-PGF_{2α} binding and function. The first amino acid selected within C-EL2 was the negatively charged Asp¹⁹³, since it represents the most critical coordination site for TPR ligands [18]. Similar to SQ29,548 and U46619, 8-iso-PGF_{2α} was found to bind Asp¹⁹³ through hydrogen bonding.

Using the tyrosine (F184Y) and alanine (F184A) mutations, we next established that Phe¹⁸⁴ coordinates with 8-iso-PGF_{2α} in a manner similar to its interaction with SQ29,548 and U46619. Specifically, it was found that Phe¹⁸⁴ binds to 8-iso-PGF_{2α} through conformationally sensitive hydrophobic forces associated with its benzene ring.

Separate experiments then determined whether amino acid residues within TM5 also play a role in the coordination between isoprostanes and TPRs. The first amino acid selected for analysis was Phe¹⁹⁶, which was subjected to either alanine (F196A) or tyrosine (F196Y) substitution. The results demonstrated that while the F196A mutant lost its Ca²⁺ response and binding capacity to [³H]8-iso-PGF_{2α}, the F196Y mutant retained both functional and binding activities. These findings indicate that Phe¹⁹⁶ plays a critical role in coordination with 8-iso-PGF_{2α}, possibly through interaction with the Phe¹⁹⁶ benzene ring.

Interestingly, however, hydrophobic interaction with Phe¹⁹⁶ was not found to be important for TPR ligand coordination with either U46619 or SQ29,548 [18], indicating that Phe¹⁹⁶ represents a unique binding site for 8-iso-PGF_{2α}. Furthermore, the present results also indicate that in contrast to U46619 [18], 8-iso-PGF_{2α} does not interact with Ser²⁰¹. Thus, even though U46619 and this isoprostane both exhibit TPR agonist activity, they possess different coordination profiles, which may explain the differences in their biological activity.

Collectively, these data demonstrate that 8-iso-PGF_{2α} interacts with TPRs at two hydrophobic sites (Phe¹⁹⁶, Phe¹⁸⁴) and one hydrogen-bonding site (Asp¹⁹³). This distribution of binding energies [29] may in part explain the substantial differences in affinities between 8-iso-PGF_{2α} and SQ29,548. Specifically, SQ29,548 which has an eightfold higher affinity than 8-iso-PGF_{2α}, also possesses more hydrogen bonding sites (three) than 8-iso-PGF_{2α} (one). On this basis, SQ29,548 would be expected to have a higher total binding energy, and a correspondingly higher affinity.

The next experiments investigated isoprostane signaling and biological function in native TPR-expressing cells, i.e., human platelets. The data revealed that 8-iso-PGF_{2α} produced

a SC response that was TPR-mediated and required the activation of ROCK. These results are consistent with an earlier study in rat smooth muscle cells demonstrating that 8-iso-PGF_{2α} can signal through the ROCK pathway [30]. On the other hand, the present experiments also demonstrated that 8-iso-PGF_{2α} did not induce platelet aggregation, which may indicate that it functions as a partial agonist at platelet TPRs, as has been previously suggested [23]. If this were the case, the enhancement of aggregation by 8-iso-PGF_{2α} (Fig. 6) should be blocked by TPR antagonism. However, it was found that SQ29,548 not only prevented 8-iso-PGF_{2α} enhancement of agonist stimulation, but also revealed 8-iso-PGF_{2α}-mediated inhibition of platelet aggregation. This finding therefore represents the first demonstration that 8-iso-PGF_{2α} exerts an inhibitory effect on human platelet function.

The next experiments investigated the mechanism of this 8-iso-PGF_{2α} inhibition. It was found that 8-iso-PGF_{2α} dose-dependently increased platelet cAMP levels, and that the AC inhibitor SQ22536 reversed its inhibition of platelet function. Taken together, these results indicate that cAMP serves as the inhibitory signaling component for 8-iso-PGF_{2α}. While the mechanism by which 8-iso-PGF_{2α} raises platelet cAMP is presently unknown, it apparently does not involve direct activation of either AC or G_{αs}, since it does not increase cAMP in HEK cells which possess both AC and G_{αs} [24]. Therefore, the most likely mechanism for 8-iso-PGF_{2α}-induced cAMP elevation would be through a Gs-coupled receptor that is present in platelets but not in HEK cells.

On this basis, we next investigated whether 8-iso-PGF_{2α} activates a known Gs-coupled prostaglandin receptor on platelets by using antagonists specific for IPR, DPR or EP₂R. It was found that none of these antagonists blocked the ability of 8-iso-PGF_{2α} to raise cAMP levels, or reversed its ability to inhibit aggregation. An alternative explanation is that the elevation in cAMP caused by 8-iso-PGF_{2α} is due to its interaction with a previously unidentified prostanoid receptor, or a novel interaction with a known Gs-coupled receptor other than IPR, DPR or EP₂R. If this were the case, platelets would be expected to possess at least two binding sites for 8-iso-PGF_{2α}.

This notion was confirmed by saturation binding experiments, which demonstrated that platelets possess two affinity sites for [³H]8-iso-PGF_{2α}, i.e., K_d = 65 nM, and K_d = 322 nM. Based on the affinity of 8-iso-PGF_{2α} in TPR expressing HEK cells (57 nM), it appears that the higher affinity-binding site represents TPR interaction, and the lower affinity site presumably represents binding to a separate platelet receptor.

Regarding the potential significance of 8-iso-PGF_{2α} signaling, it is important to note that isoprostanes can be produced

after incubation of PRP with the AC inhibitor SQ22536 (300 μM) for 45 min, PRP was treated with 50 nM SQ29,548 for 1 min, then with 1 μM 8-iso-PGF_{2α} for 3 min followed by stimulation with 15 μM TRAP-PAR1. (E) trace (a) PRP was stimulated with 15 μM TRAP-PAR1; trace (b) PRP was stimulated with 15 μM TRAP-PAR1 in the presence of 0.5 nM PGI₂; trace (c) PRP was incubated with the AC inhibitor SQ22536 (300 μM) for 45 min, and then stimulated with 15 μM TRAP-PAR1 in the presence of 0.5 nM PGI₂. (F) trace (a) PRP was stimulated with 10 μM ADP; trace (b) PRP was treated with 50 nM SQ29,548 for 1 min, then with 1 μM 8-iso-PGF_{2α} for 3 min prior to stimulation with 10 μM ADP; trace (c) PRP was stimulated with 10 μM ADP after incubation with the AC inhibitor SQ22536 (300 μM) for 45 min; trace (d) after incubation of PRP with the AC inhibitor SQ22536 (300 μM) for 45 min, PRP was treated with 50 nM SQ29,548 for 1 min, then with 1 μM 8-iso-PGF_{2α} for 3 min followed by stimulation with 10 μM ADP. (G) Non-transfected or WT TPR-transfected HEK cells were stimulated with 5 μM 8-iso-PGF_{2α} or 0.5 μM of the control forskolin. Results are the average (C and G), or representative of at least three different experiments (A, B, D, E, and F).

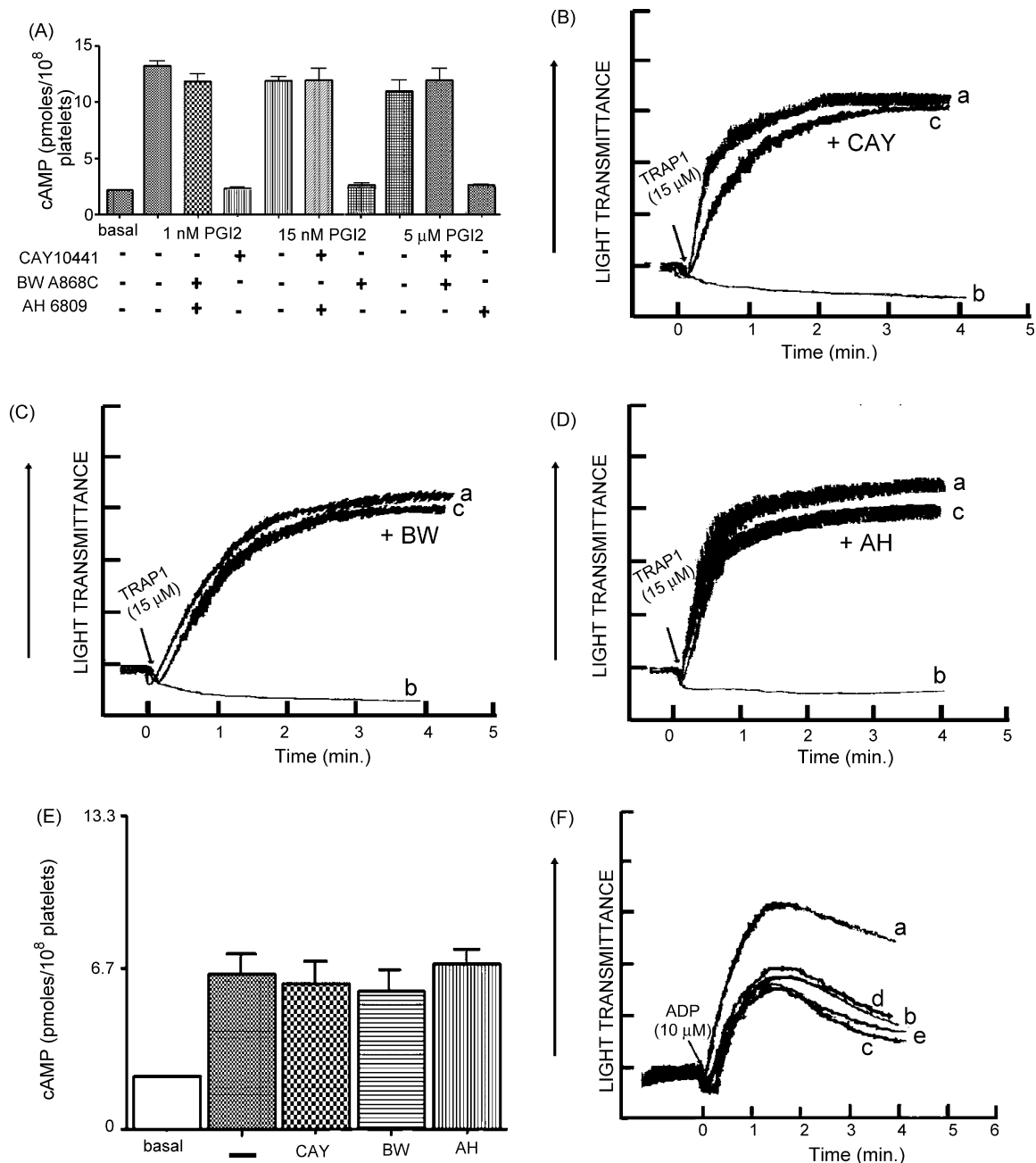


Fig. 7 – Effects of PGI₂, PGD₂, or PGE₂ on human platelet basal cAMP levels or aggregation induced by TRAP-PAR1 in the presence or absence of antagonists specific for IPR, DPR, EP₂R; and effects of 8-iso-PGF_{2α} on human platelet basal cAMP levels or ADP-induced aggregation in the presence or absence of antagonists specific for IPR, DPR, EP₂R. (A) PRP was stimulated with 1 nM PGI₂, 15 nM PGD₂, or 5 μM PGE₂ in the absence or presence of the antagonists CAY10441 (IPR specific; 250 nM) or BW A868C (DPR specific, 250 nM), or AH 6809 (EP₂R specific; 2 μM). (B) trace (a) PRP was stimulated with 15 μM TRAP-PAR1; trace (b) PRP was treated with 1 nM PGI₂ for 1 min prior to stimulation with 15 μM TRAP-PAR1; trace (c) PRP was treated with the antagonist CAY10441 (IPR specific; 250 nM), followed by 1 nM PGI₂ for 1 min prior to stimulation with 15 μM TRAP-PAR1. (C) trace (a) PRP was stimulated with 15 μM TRAP-PAR1; trace (b) PRP was treated with 15 nM PGD₂ for 1 min prior to stimulation with 15 μM TRAP-PAR1; trace (c) PRP was treated with the antagonist BW A868C (DPR specific, 250 nM), followed by 15 nM PGD₂ for 1 min prior to stimulation with 15 μM TRAP-PAR1. (D) trace (a) PRP was stimulated with 15 μM TRAP-PAR1; trace (b) PRP was treated with 5 μM PGE₂ for 1 min prior to stimulation with 15 μM TRAP-PAR1; trace (c) PRP was treated with the antagonist AH 6809 (EP₂R specific; 2 μM), followed by 5 μM PGE₂ for 1 min prior to stimulation with 15 μM TRAP-PAR1. (E) PRP was stimulated with 5 μM 8-iso-PGF_{2α} in the absence or presence of either the antagonist CAY10441 (IPR specific; 250 nM) or BW A868C (DPR specific, 250 nM), or AH 6809 (EP₂R specific; 2 μM). (F) trace (a) PRP was stimulated with 10 μM ADP; trace (b) PRP was treated with 50 nM SQ29,548 for 1 min, then with 1 μM 8-iso-PGF_{2α} for 3 min prior to stimulation with 10 μM ADP; trace (c) PRP was treated with 50 nM SQ29,548 for 1 min, then with

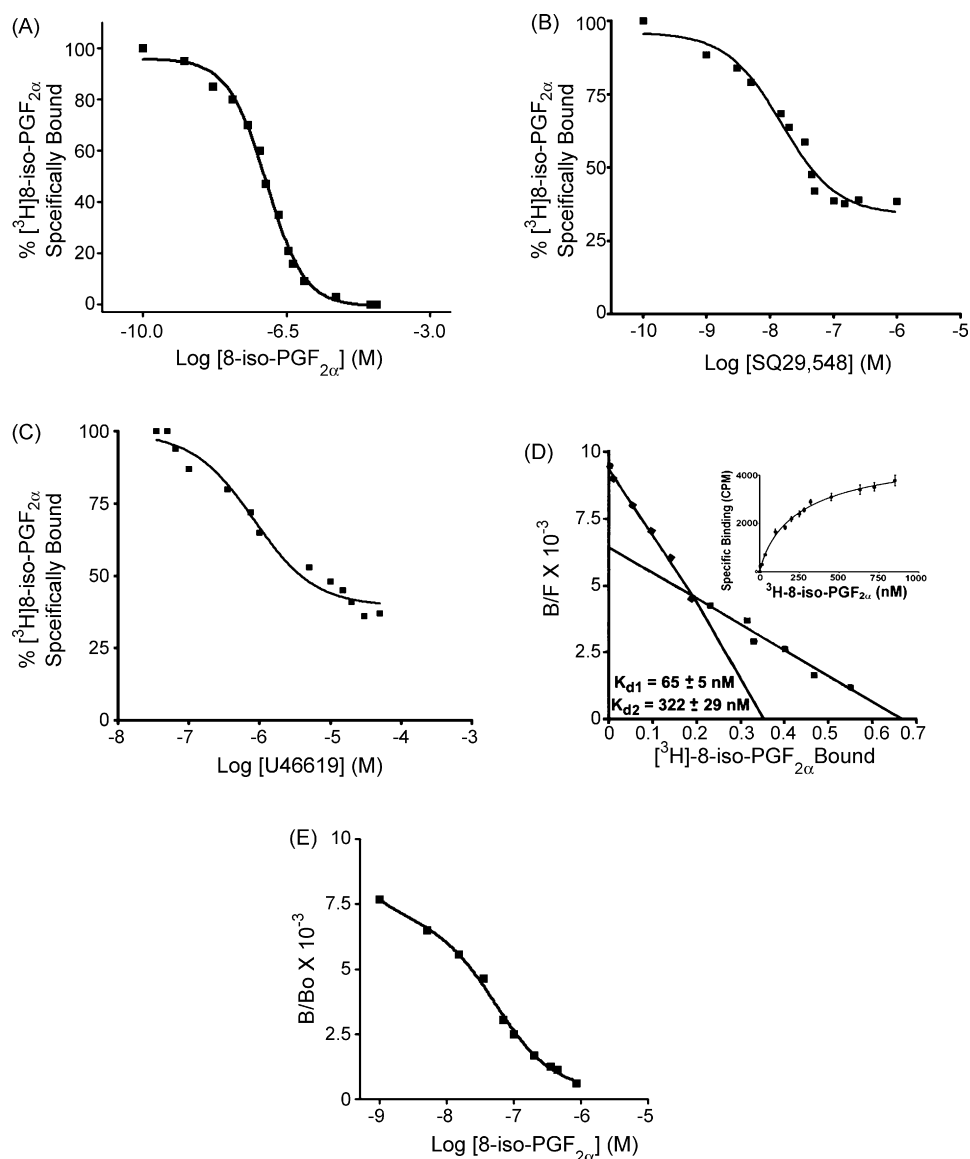


Fig. 8 – Displacement and saturation binding curves for $[^3\text{H}]8\text{-iso-PGF}_{2\alpha}$ in intact platelets. (A) Homologous displacement curve of 35 nM $[^3\text{H}]8\text{-iso-PGF}_{2\alpha}$ with increasing concentrations of the non-radiolabeled 8-iso-PGF_{2α} (0.1 nM–50 μM). (B) Binding displacement of 35 nM $[^3\text{H}]8\text{-iso-PGF}_{2\alpha}$ with increasing concentrations of SQ29,548 (0.1–1000 nM). (C) Binding displacement of 35 nM $[^3\text{H}]8\text{-iso-PGF}_{2\alpha}$ with increasing concentrations of U46619 (0.035–50 μM). (D) Saturation binding of $[^3\text{H}]8\text{-iso-PGF}_{2\alpha}$ to intact platelets analyzed by Scatchard plotting (inset shows the saturation binding data isotherm). The dissociation constants were calculated by performing non-linear regression analysis of the saturation binding data and correspond to 65 and 322 nM. (E) A B/B_0 versus Log $[8\text{-iso-PGF}_{2\alpha}]$ representation of the $[^3\text{H}]8\text{-iso-PGF}_{2\alpha}$ binding data fitted with a two-site model, which was favored by the F-test. Results are the average of at least three different experiments in each case.

in vivo at levels that are several orders of magnitude higher than classical prostaglandins/thromboxanes [2]. Consequently, the biological effects of these signaling pathways could substantially impact cellular function *in vivo*. Further-

more, it is known that the *in vivo* levels of isoprostanes can be enhanced by the presence of vascular disease [31], and there is evidence suggesting that these levels can also be elevated by aspirin (ASA) treatment [4]. Therefore, the overall contribu-

1 μM 8-iso-PGF_{2α} for 3 min prior to stimulation with 10 μM ADP in the presence of the antagonist CAY10441 (IPR specific; 250 nM); trace (d) PRP was treated with 50 nM SQ29,548 for 1 min, then with 1 μM 8-iso-PGF_{2α} for 3 min prior to stimulation with 10 μM ADP in the presence of the antagonist BW A868C (DPR specific, 250 nM); trace (e) PRP was treated with 50 nM SQ29,548 for 1 min, then with 1 μM 8-iso-PGF_{2α} for 3 min prior to stimulation with 10 μM ADP in the presence of the antagonist AH 6809 (EP₂R specific; 2 μM). Results are the average (A and E), or representative of at least three different experiments (B, C, D and F).

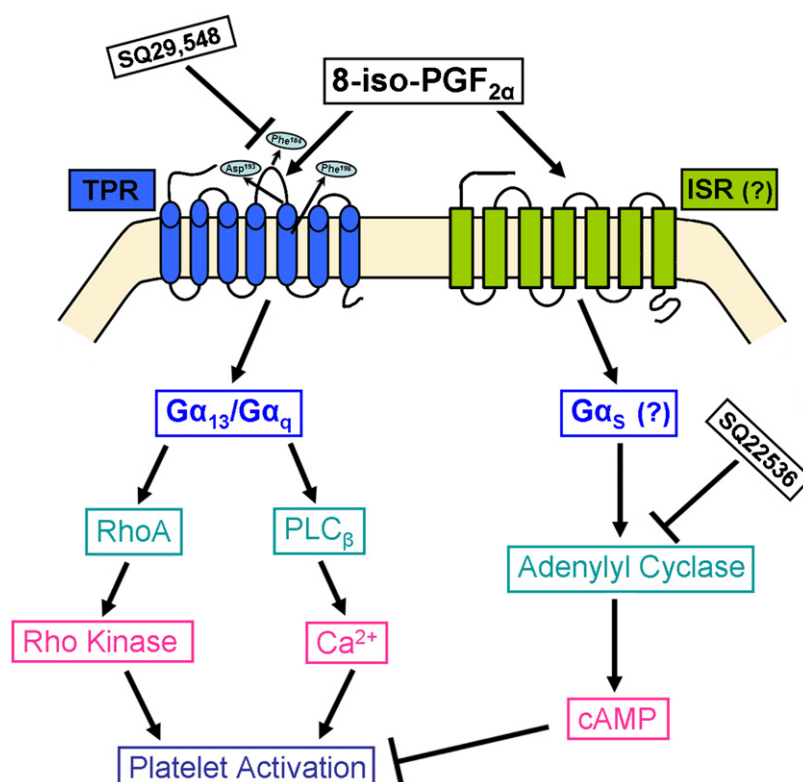


Fig. 9 – Schematic representation of the proposed signaling pathways for 8-iso-PGF_{2α}-mediated modulation of human platelet function.

tions of isoprostane signaling *in vivo* may not only be modulated by the state of vascular disease, but may also be determined by a therapeutic agent commonly used to prevent thrombosis. Thus, by blocking TXA₂ synthesis, ASA appears to facilitate increased isoprostane production, which in turn, may alter the anti-thrombotic effects of ASA itself. Based on these considerations, it might be predicted that concurrent therapy with ASA plus a TPR antagonist would be more beneficial than therapy with ASA alone. Specifically, under these conditions, the isoprostane stimulatory effects would be blocked, while its inhibitory effects would be promoted.

In summary, the present studies have provided the first comprehensive investigation of 8-iso-PGF_{2α} coordination with human TPRs, and have identified a novel signaling mechanism/biological function for 8-iso-PGF_{2α} in human blood platelets (Fig. 9). Specifically, these results have identified three key amino acids (Phe¹⁸⁴, Asp¹⁹³ and Phe¹⁹⁶) in TPRs that bind to 8-iso-PGF_{2α}, and defined the nature of the molecular forces which appear to be involved in these interactions. In addition, these studies demonstrated that Phe¹⁹⁶ serves as a unique amino acid coordination site for 8-iso-PGF_{2α}. Our findings have also resolved previous inconsistencies concerning the signaling mechanisms/functions of isoprostanes in human platelets. In this regard, our results indicate that 8-iso-PGF_{2α} signaling is a composite of two separate pathways with opposing biological activities. While the first pathway is stimulatory and TPR-mediated, the second is inhibitory and associated with increased platelet cAMP levels. The existence of these independent pathways is further supported by the

finding that platelets possess TPR-dependent and TPR-independent binding sites for 8-iso-PGF_{2α}. Finally, these collective data suggest that the mechanism by which 8-iso-PGF_{2α} increases cAMP and inhibits platelet function is either through a novel G_{αs}-coupled isoprostane receptor (ISR), or through a novel interaction with a known G_{αs}-coupled receptor.

Acknowledgments

This work was supported in part by a grant from the National Institutes of Health HL23540-24 (to G.C.L.). F.T.K. is a recipient of a predoctoral fellowship from the American Heart Association (Grant 0515533Z). The authors would like to thank Dr. Yee-Kin Ho for his valuable comments and analysis of the data, and Lanlan Dong for technical assistance.

This work has been approved by Ethics Committee at the University of Illinois at Chicago.

REFERENCES

- [1] Roberts 2nd LJ, Fessel JP. The biochemistry of the isoprostane, neuroprostane, and isofuran pathways of lipid peroxidation. *Chem Phys Lipids* 2004;128:173–86.
- [2] Morrow JD, Hill KE, Burk RF, Nammour TM, Badr KF, Roberts 2nd LJ. A series of prostaglandin F₂-like compounds are produced *in vivo* in humans by a non-cyclooxygenase, free

- radical-catalyzed mechanism. *Proc Natl Acad Sci USA* 1990;87:9383–7.
- [3] Jourdan KB, Mitchell JA, Evans TW. Release of isoprostanes by human pulmonary artery in organ culture: a cyclooxygenase and nitric oxide dependent pathway. *Biochem Biophys Res Commun* 1997;233:668–72.
 - [4] Mobert J, Becker BF. Cyclooxygenase inhibition aggravates ischemia-reperfusion injury in the perfused guinea pig heart: involvement of isoprostanes. *J Am Coll Cardiol* 1998;31:1687–94.
 - [5] Cayatte AJ, Du Y, Oliver-Krasinski J, Lavielle G, Verbeuren TJ, Cohen RA. The thromboxane receptor antagonist S18886 but not aspirin inhibits atherosclerosis in apo E-deficient mice: evidence that eicosanoids other than thromboxane contribute to atherosclerosis. *Arterioscler Thromb Vasc Biol* 2000;20:1724–8.
 - [6] Pratico D, Rokach J, Lawson J, FitzGerald GA. F2-isoprostanes as indices of lipid peroxidation in inflammatory diseases. *Chem Phys Lipids* 2004;128:165–71.
 - [7] Delanty N, Reilly MP, Pratico D, Lawson JA, McCarthy JF, Wood AE, et al. 8-epi PGF2 alpha generation during coronary reperfusion. A potential quantitative marker of oxidant stress in vivo. *Circulation* 1997;95:2492–9.
 - [8] Markesbery WR, Kryscio RJ, Lovell MA, Morrow JD. Lipid peroxidation is an early event in the brain in amnesic mild cognitive impairment. *Ann Neurol* 2005;58:730–5.
 - [9] Brault S, Martinez-Bermudez AK, Roberts 2nd J, Cui QL, Fragoso G, Hemdan S, et al. Cytotoxicity of the E(2)-isoprostane 15-E(2t)-IsoP on oligodendrocyte progenitors. *Free Radic Biol Med* 2004;37:358–66.
 - [10] Audoly LP, Rocca B, Fabre JE, Koller BH, Thomas D, Loeb AL, et al. Cardiovascular responses to the isoprostanes iPF(2alpha)-III and iPE(2)-III are mediated via the thromboxane A(2) receptor in vivo. *Circulation* 2000;101:2833–40.
 - [11] Morrow JD, Minton TA, Roberts 2nd LJ. The F2-isoprostane, 8-epi-prostaglandin F2 alpha, a potent agonist of the vascular thromboxane/endoperoxide receptor, is a platelet thromboxane/endoperoxide receptor antagonist. *Prostaglandins* 1992;44:155–63.
 - [12] Hou X, Gobeil Jr F, Peri K, Speranza G, Marrache AM, Lachapelle P, et al. Augmented vasoconstriction and thromboxane formation by 15-F(2t)-isoprostane (8-isoprostaglandin F(2alpha)) in immature pig periventricular brain microvessels. *Stroke* 2000;31:516–24. discussion 525.
 - [13] Takahashi K, Nammour TM, Fukunaga M, Ebert J, Morrow JD, Roberts 2nd LJ, et al. Glomerular actions of a free radical-generated novel prostaglandin, 8-epi-prostaglandin F2 alpha, in the rat. Evidence for interaction with thromboxane A2 receptors. *J Clin Invest* 1992;90:136–41.
 - [14] Fukunaga M, Makita N, Roberts 2nd LJ, Morrow JD, Takahashi K, Badr KF. Evidence for the existence of F2-isoprostane receptors on rat vascular smooth muscle cells. *Am J Physiol* 1993;264:C1619–24.
 - [15] Fukunaga M, Yura T, Grygorczyk R, Badr KF. Evidence for the distinct nature of F2-isoprostane receptors from those of thromboxane A2. *Am J Physiol* 1997;272:F477–83.
 - [16] Longmire AW, Roberts LJ, Morrow JD. Actions of the E2-isoprostane, 8-ISO-PGE2, on the platelet thromboxane/endoperoxide receptor in humans and rats: additional evidence for the existence of a unique isoprostane receptor. *Prostaglandins* 1994;48:247–56.
 - [17] Pratico D, Smyth EM, Violi F, FitzGerald GA. Local amplification of platelet function by 8-Epi prostaglandin F2alpha is not mediated by thromboxane receptor isoforms. *J Biol Chem* 1996;271:14916–24.
 - [18] Khasawneh FT, Huang JS, Turek JW, Le Breton GC. Differential mapping of the amino acids mediating agonist and antagonist coordination with the human thromboxane A2 receptor protein. *J Biol Chem* 2006;281:26951–65.
 - [19] Kattelman EJ, Venton DL, Le Breton GC. Characterization of U46619 binding in unactivated, intact human platelets and determination of binding site affinities of four TXA2/PGH2 receptor antagonists (13-APA, BM 13.177, ONO 3708 and SQ 29,548). *Thromb Res* 1986;41:471–81.
 - [20] Michal F, Born GV. Effect of the rapid shape change of platelets on the transmission and scattering of light through plasma. *Nat New Biol* 1971;24:220–2.
 - [21] Gilman AG. A protein binding assay for adenosine 3':5'-cyclic monophosphate. *Proc Natl Acad Sci USA* 1970;67:305–12.
 - [22] Hung SC, Ghali NI, Venton DL, Le Breton GC. Specific binding of the thromboxane A2 antagonist 13-azaprostanoic acid to human platelet membranes. *Biochim Biophys Acta* 1983;728:171–8.
 - [23] Yin K, Halushka PV, Yan YT, Wong PY. Antiaggregatory activity of 8-epi-prostaglandin F2 alpha and other F-series prostanoids and their binding to thromboxane A2/prostaglandin H2 receptors in human platelets. *J Pharmacol Exp Ther* 1994;270:1192–6.
 - [24] Ulloa-Aguirre A, Uribe A, Zarinan T, Bustos-Jaimes I, Perez-Solis MA, Dias JA. Role of the intracellular domains of the human FSH receptor in G α s protein coupling and receptor expression. *Mol Cell Endocrinol* 2007;260–262:153–62.
 - [25] Clark RD, Jahangir A, Severance D, Salazar R, Chang T, Chang D, et al. Discovery and SAR development of 2-(phenylamino) imidazolines as prostacyclin receptor antagonists [corrected]. *Bioorg Med Chem Lett* 2004;14:1053–6.
 - [26] Liu YJ, Jackson DM, Blackham A. Effects of BW A868C, a selective prostaglandin DP receptor antagonist, in dog isolated vascular preparations. *Eur J Pharmacol* 1996;303:187–92.
 - [27] Meja KK, Barnes PJ, Giembycz MA. Characterization of the prostanoid receptor(s) on human blood monocytes at which prostaglandin E2 inhibits lipopolysaccharide-induced tumour necrosis factor-alpha generation. *Br J Pharmacol* 1997;122:149–57.
 - [28] Huang JS, Dong L, Le Breton GC. Mass-dependent signaling between G protein coupled receptors. *Cell Signal* 2006;18:564–76.
 - [29] Bohm HJ. Prediction of binding constants of protein ligands: a fast method for the prioritization of hits obtained from de novo design or 3D database search programs. *J Comput Aided Mol Des* 1998;12:309–23.
 - [30] Yi SL, Kantores C, Belcastro R, Cabacungan J, Tanswell AK, Jankov RP. 8-Isoprostane-induced endothelin-1 production by infant rat pulmonary artery smooth muscle cells is mediated by Rho-kinase. *Free Radic Biol Med* 2006;41:942–9.
 - [31] Cracowski JL, Durand T, Bessard G. Isoprostanes as a biomarker of lipid peroxidation in humans: physiology, pharmacology and clinical implications. *Trends Pharmacol Sci* 2002;23:360–6.